PAPER

High power semiconductor laser array with single-mode emission

High power semiconductor laser array with single-mode emission

Peng Jia(贾鹏)[1], Zhi-Jun Zhang(张志军)[4], Yong-Yi Chen(陈泳屹)[1,5,†], Zai-Jin Li(李再金)[2,‡], Li Qin(秦莉)[1], Lei Liang(梁磊)[1], Yu-Xin Lei(雷宇鑫)[1], Cheng Qiu(邱橙)[1], Yue Song(宋悦)[1], Xiao-Nan Shan(单肖楠)[1], Yong-Qiang Ning(宁永强)[1], Yi Qu(曲轶)[2], and Li-Jun Wang(王立军)[1,3]

[1] *State Key Laboratory of Luminescence and Application, Changchun Institute of Optics, Fine Mechanics and Physics, Chinese Academy of Sciences, Changchun* 130033, *China*

[2] *Academician Team Innovation Center of Hainan Province, Key Laboratory of Laser Technology and Optoelectronic Functional Materials of Hainan Province, School of Physics and Electronic Engineering, Hainan Normal University, Haikou* 571158, *China*

[3] *Peng Cheng Laboratory No.* 2, *Xingke* 1*st Street, Nanshan, Shenzhen, China*

[4] *Liaoning Institute of Science and Technology, Anshan* 114051, *China*

[5] *Jlight Semiconductor Technology Co., Ltd., Changchun* 130033, *China*

(Received 13 September 2021; revised manuscript received 5 November 2021; accepted manuscript online 6 November 2021)

The semiconductor laser array with single-mode emission is presented in this paper. The 6-μm-wide ridge waveguides (RWGs) are fabricated to select the lateral mode. Thus the fundamental mode of laser array can be obtained by the RWGs. And the maximum output power of single-mode emission can reach 36 W at an injection current of 43 A, after that, a kink will appear. The slow axis (SA) far-field divergence angle of the unit is 13.65°. The beam quality factor M^2 of the units determined by the second-order moment (SOM) method, is 1.2. This single-mode emission laser array can be used for laser processing.

Keywords: semiconductor laser arrays, single-mode, high power, high beam quality

PACS: 42.55.Px, 78.55.Cr, 78.67.De, 42.60.Pk **DOI:** 10.1088/1674-1056/ac373d

1. Introduction

High-power single-mode semiconductor lasers and arrays have the advantages of high power, high wall-plug efficiency, and single-mode operation.[1–4] The single-mode arrays are required in the applications of dense wavelength division multiplexing, telecommunication, and laser processing.[5–8]

Recently, many methods have been reported to realize the single-mode emission semiconductor laser arrays. The laser arrays with single-mode emission are reported by BOOKHAM company, the ridge waveguide with 5 μm in width was utilized to obtain single-mode operation.[9] The slab-coupled optical waveguide laser (SCOWL) integrated deep etching ridge waveguide array is used to realize a single-mode emission, which is reported by MIT.[10,11] The large size N waveguide layer is designed to reduce the optical limiting factor in P waveguide layer, which will increase the maximum output power. However, the SCOWL has the defect of low conversion efficiency. The FBH institute and TRUMPF laser company reported a single-mode laser array based on an asymmetric waveguide epitaxial structure.[12,13] A high-power laser array with single-mode emission was proposed by II–VI company, which was processed by facet surface passivation technology.[14]

In this paper, we show a semiconductor laser array with single-mode emission, and the single lateral mode is determined mainly by the 6μm-wide ridge waveguides. The ridge waveguides can support the fundamental mode operation, which is analyzed by the single-mode cutoff condition. And the unit spacing is optimized by using a temperature distribution model. A single-mode laser array is implemented with output power of 37.5 W and a wall-plug efficiency of 56.2%, and near diffraction limit beam quality factor M^2 can arrive at 1.2.

2. Device design and fabrication

High-power laser arrays with single-mode emission are presented in this paper as shown in Fig. 1. The epitaxial wafer was prepared by metal–organic chemical vapor deposition (MOCVD), which was composed of a single InGaAs quantum well in the active region at a wavelength of 975 nm. The fundamental mode was obtained by 6-μm-wide ridge waveguides in an array serving as a mode filter. And the units were separated by isolation grooves to eliminate the crosstalk between carrier and photonics.

A two-dimensional (2D) model was calculated by commercial software COMSOL Multiphysics for obtaining the geometric parameters of single-mode ridge waveguide, including width and depth of the waveguide mesa as shown in Fig. 2. In Fig. 2(a), we find that the fundamental mode is distributed mainly under a 6-μm-wide mesa with injection

†Corresponding author. E-mail: chenyy@ciomp.ac.cn
‡Corresponding author. E-mail: lizaijin@126.com

currents, which will achieve the lowest internal losses and threshold gain. Figure 2(b) shows that the high-order mode is transmitted off the mesa, which will be rapidly absorbed or scattered out.[15,16] Thus the high-order modes are eliminated, and single-mode emission laser arrays is realized as shown in Fig. 1.[17]

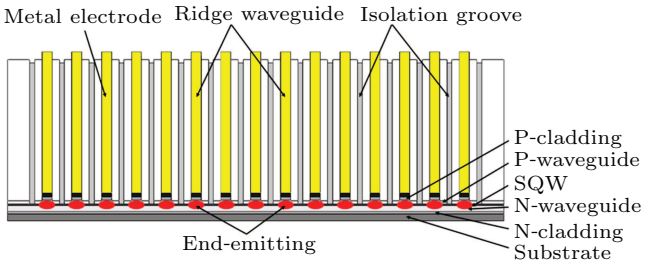

Fig. 1. Schematic diagram of single-mode laser arrays.

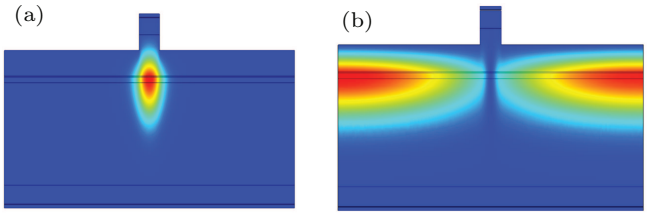

Fig. 2. The 2D color mapping of intensity distribution of (a) fundamental mode and (b) high-order mode in 6-μm-wide ridge waveguide with etching depth fixed at 1.2 μm.

The spectral and beam quality characteristics of single-mode arrays would be affected significantly by the waste heat. A laser array temperature distribution model was utilized to analyze the temperature of laser units with different unit spacing in the laser array. From Fig. 3, we can find that the top temperature of array rapidly rises with the decreases of the unit spacing, and the temperature of the central units is significantly higher than that of the edge units. It is because that when the waste heat power values of four arrays are all 30 W in our model, the less the spacing is, the more unlikely the waste to be dissipated is. Thus the temperature will decrease with the increase of unit spacing. Yet when the unit spacing increases to a certain level, say, from 72 μm to 96 μm, the top temperature decreases slower. This is because when the unit spacing is enlarged to a certain extent, the heat dissipation rate remains almost unchanged. Yet, larger unit spacing will enlarge the array's size and will reduce the yield of the total useful arrays.

Figure 4 shows that the temperature difference ΔT between core and periphery region is the largest in the laser array with 24-μm-wide unit spacing, which will decrease as the spacing increases from 24 μm to 96 μm. The slope of the change in temperature and ΔT gradually decrease, respectively. Specially, the temperature difference decreases from 1.95 K to 0.89 K as the unit spacing increases from 24 μm to 48 μm. This is mainly because, when the laser unit spacing is small, the thermal crosstalk between each unit and the remaining units increases, which is caused by the unit self-heat accumulation in the array. The thermal crosstalk effect between each unit would be enhanced as the laser unit spacing reduces, and the temperature of each unit is raised by heat generated from adjacent units. The more the units in the same length of array, the more serious the thermal crosstalk of adjacent units is, which will raise the temperature of laser array, and the electro-optical conversion efficiency will drop at high temperature.

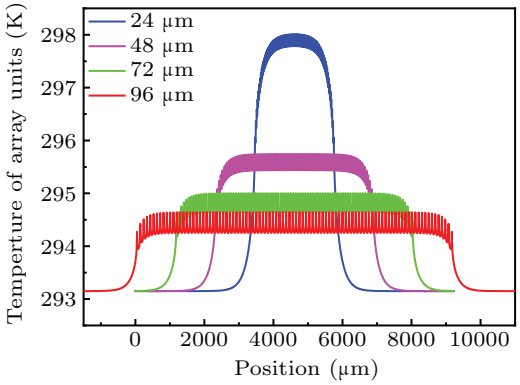

Fig. 3. Thermal distribution of single-mode laser arrays with different unit spacing from 24 μm to 96 μm.

Because of temperature difference between the core and edge units, the gain spectrum will also shift. The spectrum of the total array will widen as the number of units increases. Thus the unit spacing of laser arrays cannot be too small. At the same time, to ensure the output power, the fill factor should not be too small, and therefore the unit spacing should not be too large. Thus we determine the unit center spacing of the single-mode laser array to be 48 μm.

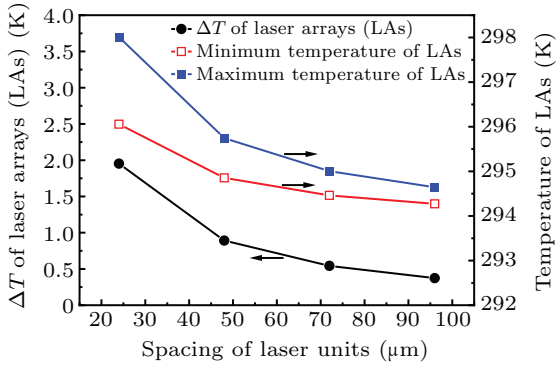

Fig. 4. Temperature difference between core and periphery position in single-mode laser arrays with different unit spacings.

The wafer was epitaxially grown by the MOCVD, which was composed of a single InGaAs quantum well, $Al_xGa_{1-x}As$ optical waveguide, and optical confine layers. The wafer had an asymmetric large optical cavity (LOC) waveguide structure consisting of an 800-nm-thick P optical waveguide and an 1200-nm-thick N optical waveguide. The LOC waveguide can enlarge the vertical mode volume and reduce the vertical far-field divergence angle at the same time, and the optical catastrophic damage threshold of the device will be increased.

The ridge waveguides and isolation grooves were determined by using i-line lithography and dry etching, and the width of waveguides and grooves were 6 μm and 12 μm, respectively, the etching depth of waveguides and grooves were 1.2 μm and 2 μm as shown in Fig. 1. After that, SiO_2 film was deposited on surface of wafer by using PECVD to isolate injection current diffusion. The metal electrodes were grown respectively, on the P and N surfaces of the chip by using metal magnetron sputtering technique. Finally, the chip was cleaved and 98% reflective coating was deposited on one facet of laser arrays, then 1.5% anti-reflective coating was deposited on the other facet. The laser arrays with the footprint of 2 mm×4.8 mm were mounted p-side up on a micro-channel cooler (MCC) through using indium solder.

3. Results and discussion

The devices are mounted on water-cooled bases with a cooling water temperature of 18 °C, which are tested under continuous injection current from 0 A to 45 A. The continuous wave (CW) power and voltage characteristics are obtained by Newport 843-R power meter and thermopile sensor, and the wall-plug efficiency (WPE) is also calculated as shown in Fig. 5. The spectra are measured by YOKOGAWA AQ6370C optical spectrum analyzer using an integrating sphere and a 100-μm-core-diameter fiber with a 0.02-nm resolution, which means that the test error is ±0.02 nm. The output spectrum at an injection current of 20 A is shown in Fig. 6. The far-field radiation patterns are obtained by using Ophir-Spiricon SP620U camera as indicated in Fig. 7.

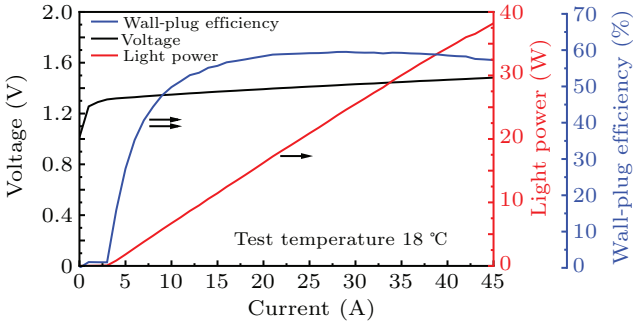

Fig. 5. CW power and voltage characteristics of our single-mode laser arrays.

Figure 5 shows that the maximum power of laser array is 37.5 W at an injection current of 45 A, and the threshold current and slope efficiency are 3 A and 0.892 W/A, respectively. The wall-plug efficiency of 56.2% is obtained at an injection current of 45 A, and the maximum WPE is 58.4% at 29 A. A kink of power occurs at 43 A, which is a mode jumping causing by thermal reversal. The array power with no kink is 36 W, thus the unit power is 0.36 W at an injection current of 0.29 A.

The device operates in multi-longitudinal mode with a wavelength of 973.3 nm and a spectral full width at half maximum (FWHM) of 0.76 nm at 20-A current injection as shown in Fig. 6. And the spectral linewidth with 95% power is 4.37 nm, which is close to the spectral linewidths of traditional array devices.

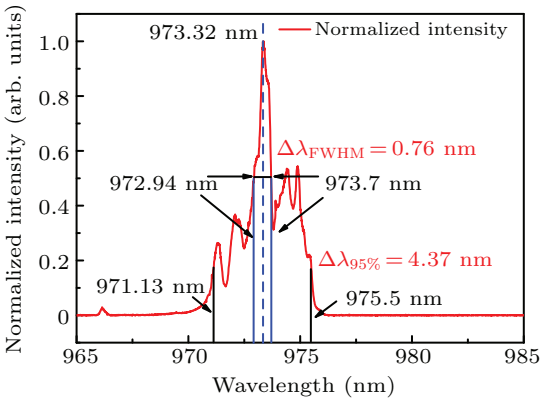

Fig. 6. Optical spectrum of our single-mode laser arrays at injection current of 20 A.

The second-order moment method is utilized to analyze the slow axis (SA) far-field divergence angle of the device, according to the standard ISO 11146–2005.[18] The full angle of far-field divergence containing 95% optical power at an injection current of 45 A is 13.65°, when the spacing of 100 mm between laser array facet and observation screen, which is shown in Fig. 7. The far-field radiation pattern is of nearly Gaussian beam. This is due to the small spacing between the luminescent units and the superposition and coupling of the Gaussian beams in each unit in the propagation process, so that the far-field distribution is near Gaussian.

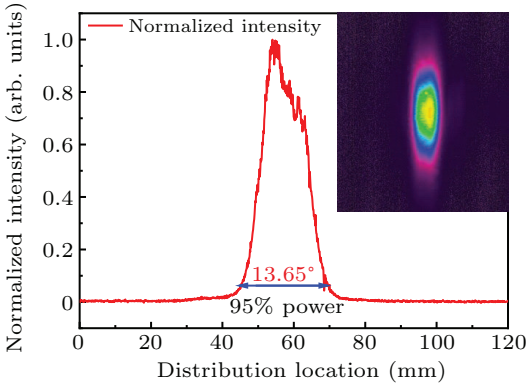

Fig. 7. Far-field radiation pattern and intensity distribution of single-mode laser array at injection current of 45 A.

The SA divergence angle of laser array is larger than that of single-mode laser emitter, thus we can determine SA angle of the unit to be 13.65°, approximatively. And the waist radius of output beam is equivalent to the width of ridge waveguide, which is 6 μm. Thus the beam quality factor M^2 of the units can be determined by the SOM method to be 1.2 at an injection current of 45 A.

4. Conclusions

A single-mode operation of semiconductor laser array is reported. The stable single-mode emission can be kept under

43 A. And the maximum output power of single-mode operation can reach 36 W. The beam quality factor of $M^2 = 1.2$ at an injection current of 45 A is obtained. The fundamental mode originates mainly from the ridge waveguide mode selection. The reported single-mode laser arrays are fabricated by I line lithography and dry etch technology. And this method provides a significant cost advantage and excellent beam quality performance compared with other methods.

Acknowledgements

Project supported by the National Science and Technology Major Project of China (Grant Nos. 2018YFB0504600 and 2017YFB0405102), the Frontier Science Key Program of the President of the Chinese Academy of Sciences (Grant No. QYZDY-SSW-JSC006), the Pilot Project of the Chinese Academy of Sciences (Grant No. XDB43030302), the National Natural Science Foundation of China (Grant Nos. 62090051, 62090052, 62090054, 11874353, 61935009, 61934003, 61904179, 61727822, 61805236, 62004194, and 61991433), the Science and Technology Development Project of Jilin Province, China (Grant Nos. 20200401062GX, 202001069GX, 20200501006GX, 20200501007GX, 20200501008GX, and 20190302042GX), the Key Research and Development Project of Guangdong Province, China (Grant No. 2020B090922003), the Equipment Pre-research, China (Grant No. 2006ZYGG0304), the Special Scientific Research Project of the Academician Innovation Platform in Hainan Province, China (Grant No. YSPTZX202034), and the Dawn Talent Training Program of CIOMP, China.

References

[1] Pietrzak A, Wenzel H, Crump P, Bugge B, Fricke J, Spreemann M and Erbert G 2012 *IEEE J. Quantum. Electron* **48** 568

[2] Guo W H, Lu Q Y, Nawrocka M, Abdullaev A, O'Callaghan J and Donegan J F 2013 *Opt. Express* **21** 10215

[3] Ma D Z, Chen Y Y, Lei Y X, Jia P, Gao F, Zeng Y G, Liang L, Song Y, Ruan C K, Liu X, Qin L, Ning Y Q and Wang L J 2021 *Chin. Phys. B* **30** 050505

[4] Zhou D B, Liang S, Han L S, Zhao L J and Wang W 2017 *Chin. Phys. Lett.* **34** 034204

[5] Smistrup K, Norregaard J, Mironov A, Bro T H, Bilenberg B, Nielsen T, Eriksen J, Thilsted A H, Hansen O and Kristensen A 2014 *Microelectron. Eng.* **123** 149

[6] Fedorov V Y and Tzortzakis S 2020 *Light: Sci. Appl.* **9** 186

[7] Huang R K, Chann B, Missaggia L J, Augst S J, Connors M K, Turner G W, Rubio A S, Donnelly J P, Hostetler J L, Miester C and Dorsch F 2009 *Proceedings of SPIE Conference on Novel in-Plane Semiconductor Lasers VIII*, January 26–29, 2009, San Jose, USA, p. 72301G

[8] Zhao Y, Zhang J C, Jia Z W, Liu Y H, Zhuo N, Zhai S Q, Liu F Q and Wang Z G 2016 *Chin. Phys. Lett.* **33** 124201

[9] Lichtenstein N, Manz Y, Mauron P, Fily A, Arlt S, Thies A, Schmidt B, Muller J, Pawlik S, Sverdlov B and Harder C 2004 *19th IEEE International Semiconductor Laser Conference*, September 21–25, 2004, Matsue, Japan, p. 45

[10] Huang R K, Missaggia L J, Donnelly J P, Harris C T and Turner G W 2005 *IEEE Photon. Tech. Lett.* **17** 959

[11] Donnelly J P, Huang R K, Walpole J N, Missaggia L J, Harris C T, Plant J J, Bailey R J, Mull D E, Goodhue W D and Turner G W 2003 *IEEE J. Quantum. Electron* **39** 289

[12] Müller J, Bättig R, Beer V, Blumer C, Brunner R, Telkkälä J and Wolf J 2019 *Proceedings of SPIE High-power Diode Laser Technolog XVII*, February 03–05, 2019, San Francisco, USA, p. 10900

[13] Wilkens M, Wenzel H, Fricke J, Maabdorf A, Ressel P, Strohmaier S, Knigge A, Erbert G and Trankle G 2018 *IEEE Photon. Tech. Lett.* **30** 545

[14] Strohmaier S G, Erbert G, Rataj T, Meissner-Schenk A H, Loyo-Maldonado V, Carstens C, Zimer H, Schmidt B, Kaul T, Karow M M, Wilkens M and Crump P 2018 *Proceedings of SPIE High-Power Diode Laser Technology XVI*, January 29–30, 2018, San Francisco, USA, p. 10514

[15] Sumpf B, Fricke J, Maiwald M, Mueller A, Ressel P, Bugge F, Erbert G and Traenkle G 2014 *Semicond. Sci. Technol.* **29** 045025

[16] Müller A, Fricke J, Brox O, Erbert G and Sumpf B 2016 *Semicond. Sci. Technol.* **31** 125011

[17] Chuan S L 2009 *Physics of Photonic Devices-Second Edition* (Chichester: John Wiley and Sons) p. 261

[18] Washington: International Standards Organization 2005 *ISO* 11146-1, *Lasers and laser-related equipment — Test methods for laser beam widths, divergence angles and beam propagation ratios — Part* 1*: Stigmatic and simple astigmatic beams*